# The OptoTracker project

Andrea Celentano

INFN-Genova

September 24, 2015

## The OptoTracker project

### Project goal

Investigate a new approach to charged particle tracking:
use the optical signal from a scintillating material, exploiting the light as information carrier.

Proposed technology:

- Collect the scintillation light emitted by organic or inorganic scintillators along the primary particle path with pixelized photo-detectors.
- Measure the hit charge and time for each pixel.
- Perform 3D-tracking by using a sophisticated reconstruction algorithm implementing the time-reversal imaging.

**Main deliverable:** design, construct, and test a working small-scale demonstrator.

# Charged particles tracking

## Traditional approach to charged particles tracking (TPC detectors)

The "traditional" approach exploits the ionization process:

- The primary particle produces ionization along the path.
- Secondary $e^-$ and ions drift in an external $\vec{E}$ field toward the collecting region.

Track reconstruction:

- Transverse coordinates measured using a pixelized readout.
- Drift coordinate determined by measuring the drift time.

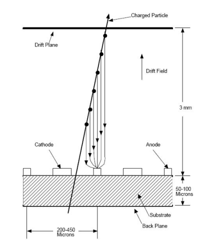


## Critical aspects of this approach:

1. Position resolution is limited by the diffusion of charge carriers:

$$\sigma_x^2 \geq \frac{2kT}{e}\frac{L_d}{E} \quad \rightarrow \quad \text{ALICE TPC}^1\text{: } \sigma_x \simeq 1\,mm \text{ @ } L_d = 2.5\,m$$

2. Slow signal formation time limits the maximum operation rate to $O$(1-10 kHz)

[1] arXiv:1001.1950

## A new approach to the problem

### A tracking detector exploiting the light signal does not suffer these limitations

- Light is the fastest information carrier within a material: an OptoTracker is intrinsically capable of sustaining a very high rate.
- The diffusion length of the carriers (photons) in a scintillator is $O(m)$: it does not affect the position resolution in a detector with comparable dimensions.

This technology would permit to construct large-scale active-targets with enhanced particle ID and background rejection capabilities.

The design of an OptoTracker requires state-of-the-art technologies, with superior performances.

- Fast, high light yield, highly transparent scintillators.
- Highly pixelized, fast photo-detectors, sensitive to single photoelecrons: MA-PMTs, SiPMs, LA-PPDs.
- Fast, low-noise, multi-channel readout-system: TOFPET, MAROC3, PSEC4.

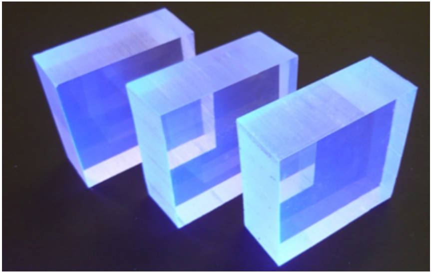

## A new approach to the problem

**A tracking detector exploiting the light signal does not suffer these limitations**

- Light is the fastest information carrier within a material: an OptoTracker is intrinsically capable of sustaining a very high rate.
- The diffusion length of the carriers (photons) in a scintillator is $O(m)$: it does not affect the position resolution in a detector with comparable dimensions.

This technology would permit to construct large-scale active-targets with enhanced particle ID and background rejection capabilities.

The design of an OptoTracker requires state-of-the-art technologies, with superior performances.

- Fast, high light yield, highly transparent scintillators.
- Highly pixelized, fast photo-detectors, sensitive to single photoelecrons: MA-PMTs, SiPMs, LA-PPDs.
- Fast, low-noise, multi-channel readout-system: TOFPET, MAROC3, PSEC4.

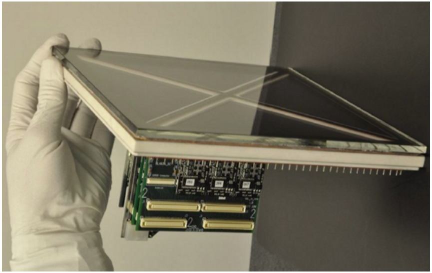

# A new approach to the problem

## A tracking detector exploiting the light signal does not suffer these limitations

- Light is the fastest information carrier within a material: an OptoTracker is intrinsically capable of sustaining a very high rate.
- The diffusion length of the carriers (photons) in a scintillator is $O(m)$: it does not affect the position resolution in a detector with comparable dimensions.

This technology would permit to construct large-scale active-targets with enhanced particle ID and background rejection capabilities.

The design of an OptoTracker requires state-of-the-art technologies, with superior performances.

- Fast, high light yield, highly transparent scintillators.
- Highly pixelized, fast photo-detectors, sensitive to single photoelecrons: MA-PMTs, SiPMs, LA-PPDs.
- Fast, low-noise, multi-channel readout-system: TOFPET, MAROC3, PSEC4.

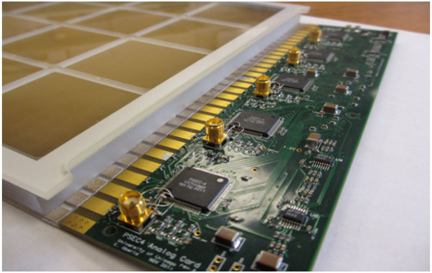

## A new approach to the problem

**A tracking detector exploiting the light signal does not suffer these limitations**

- Light is the fastest information carrier within a material: an OptoTracker is intrinsically capable of sustaining a very high rate.
- The diffusion length of the carriers (photons) in a scintillator is $O(m)$: it does not affect the position resolution in a detector with comparable dimensions.

This technology would permit to construct large-scale active-targets with enhanced particle ID and background rejection capabilities.

The design of an OptoTracker requires state-of-the-art technologies, with superior performances.

- Fast, high light yield, highly transparent scintillators.
- Highly pixelized, fast photo-detectors, sensitive to single photoelecrons: MA-PMTs, SiPMs, LA-PPDs.
- Fast, low-noise, multi-channel readout-system: TOFPET, MAROC3, PSEC4.

These technologies are available **today!**

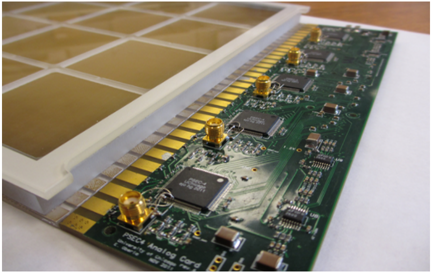

# Reconstruction algorithms: numerical approach

**Approach:** investigate the solutions developed in other fields, sharing similar issues, and adapt them to the specific problem.

## Optical Tomography

Starting point: methods used in **Optical Tomography**, based on the **Expectation-Maximization** approach. Specificity of this problem: the use of the **time information** in the reconstruction algorithm.

Reconstruction approach: discretize the system, in terms of voxels.

- Measured pixels response (including noise) → $\mathbf{g}$
- System transfer matrix → $H$
- Unknown voxels excitation → $\mathbf{x}$
- Noise → $\mathbf{n}$

$$\mathbf{g} = H \cdot \mathbf{x} + \mathbf{n}$$

## Reconstruction algorithms: numerical approach

- **Direct problem:** use MonteCarlo simulations to characterize the system matrix $H_{ij}$. “Switch on” one voxel $x_i$ at time and evaluate the corresponding pixels response $g_j$.
- **Inverse problem:** reconstruct the “image” $x_i$ from pixels response using the Moore-Penrose pseudoinverse matrix.

First results look promising:

Setup:

- Plastic scintillator cube, L=6 cm, 5x5x5 voxels
- 4 detectors on side faces, 2.4 $\times$ 4.8 cm$^2$, 8x16 pixels

Results for a central vertical trace:

- Data: pixels response for a single event
- Reconstruction: voxels excitation

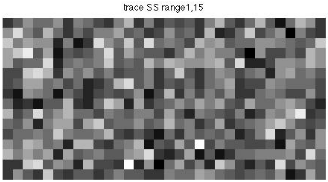

# Reconstruction algorithms: numerical approach

- **Direct problem:** use MonteCarlo simulations to characterize the system matrix $H_{ij}$. "Switch on" one voxel $x_i$ at time and evaluate the corresponding pixels response $g_j$.
- **Inverse problem:** reconstruct the "image" $x_i$ from pixels response using the Moore-Penrose pseudoinverse matrix.

First results look promising:

Setup:

- Plastic scintillator cube, L=6 cm, 5x5x5 voxels
- 4 detectors on side faces, 2.4 $\times$ 4.8 cm$^2$, 8x16 pixels

Results for a central vertical trace:

- Data: pixels response for a single event
- Reconstruction: voxels excitation

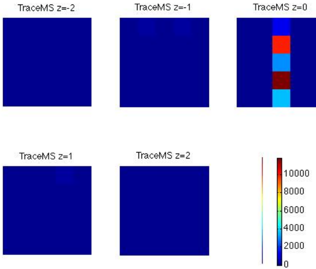

## Reconstruction algorithms: analytic approach

Second reconstruction step: use an analytic reconstruction algorithm, where the event topology is imposed a-priori (track-like or point-like), using results from the numerical approach.

- Use an analytic model to describe the light emission and propagation in the scintillator.
- Construct the Likelihood function for the pixel $p_i$ to measure $N_i$ photo-electrons at times[2] $t_i$: $\mathcal{L}_i(N_i, t_i; \vec{x})$
- Maximize the overall Likelihood function to determine the trajectory: $\mathcal{L} = \prod_i \mathcal{L}_i$

The likelihood approach permits to exploit both the **hit charge** and the **hit time** information in the reconstruction algorithm.

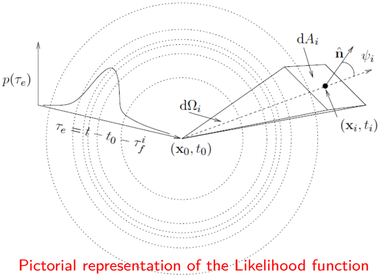


Pictorial representation of the Likelihood function for a point-like event

# Reconstruction algorithms: analytic approach. First results

Reconstruction algorithm has been tested on MonteCarlo data, to validate it (only hit-charge information included in the Likelihood so far). First results look promising.
Detector configuration: $6 \times 6 \times 6$ cm$^3$ plastic scintillator cube, 4 detectors on the lateral faces

Point-like event: $\alpha$ particle in (0.5,2.1,-1.6) cm

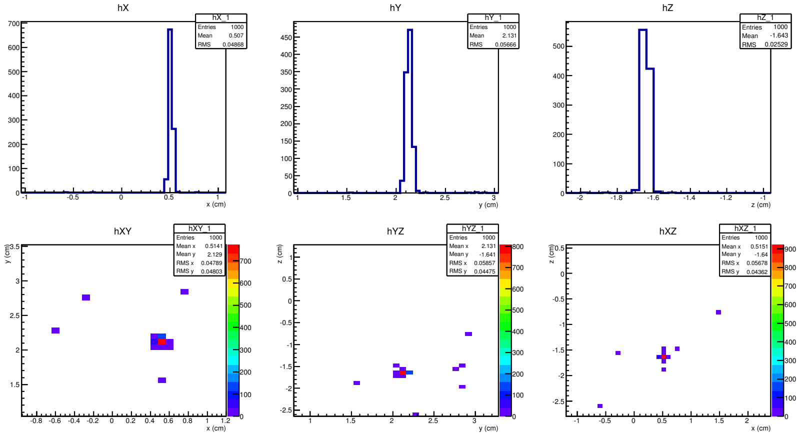

# Reconstruction algorithms: analytic approach. First results

Reconstruction algorithm has been tested on MonteCarlo data, to validate it (only hit-charge information included in the Likelihood so far). First results look promising.
Detector configuration: $6 \times 6 \times 6$ cm$^3$ plastic scintillator cube, 4 detectors on the lateral faces

Track event: $\mu$ entering in (3,0.51,0.02) cm with $\theta = 12.6°$, $\phi = 26.6°$

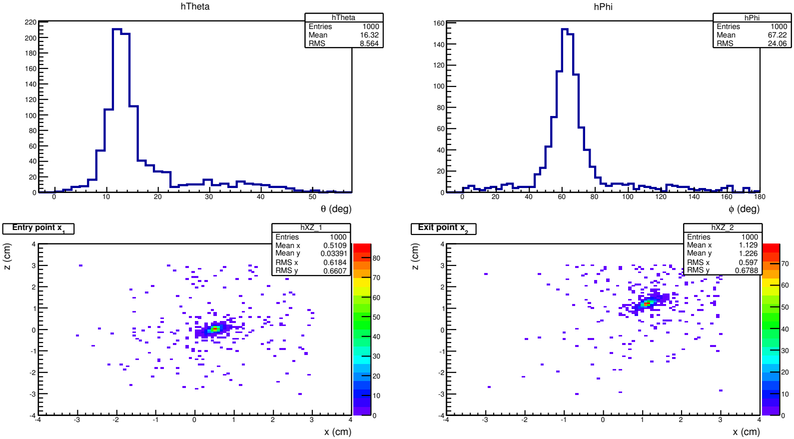

## First prototype

A first prototype, optimized for **charge measurements only**, has been designed and constructed. The response to radioactive sources has been measured.

### Goals

- Validate MC (charge part)
- Study the reconstruction direct problem

### Setup

- EJ-230 scintillator cube, 6×6×6 $cm^3$
- 2x H8500 MA-PMTs coupled to orthogonal faces
- Anti-reflection black coating
- MAROC3-based readout system, optimized for internal trigger only: OR of all channels, threshold $\simeq$ 1 phe

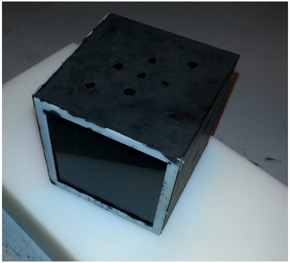

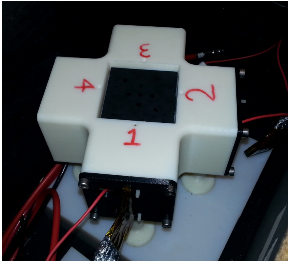

# First measurements

The prototype response to a point-like $\alpha$ radioactive source ($^{241}Am$, $E = 5.49$ MeV) placed on the top face in different positions has been measured.

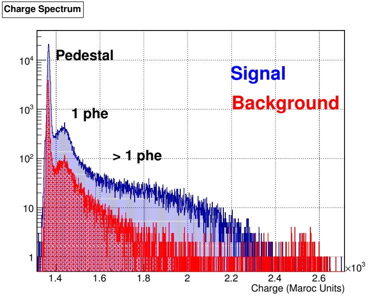


1. For each channel, the **charge** spectrum with and without the source has been measured
2. To obtain the "true" source spectrum: pedestal subtraction + background subtraction

The H8500 single phe response function is too broad to perform a charge-based event-by-event reconstruction. Instead: perform a whole-spectrum analysis.

$$< N(Q_i) > = < E > \cdot LY \cdot G_i \cdot \varepsilon_i \cdot k_i$$

Normalize to the sum of the pixel averages:

$$\frac{< N(Q_i) >}{\sum_i < N(Q_i) >} = \frac{G_i \varepsilon_i k_i}{\sum_i G_i \varepsilon_i k_i}$$ $\Rightarrow$ This can be compared with MC results for $k_i$

# First measurements

The prototype response to a point-like $\alpha$ radioactive source ($^{241}Am$, $E = 5.49$ MeV) placed on the top face in different positions has been measured.

1. For each channel, the **charge** spectrum with and without the source has been measured
2. To obtain the "true" source spectrum: pedestal subtraction + background subtraction

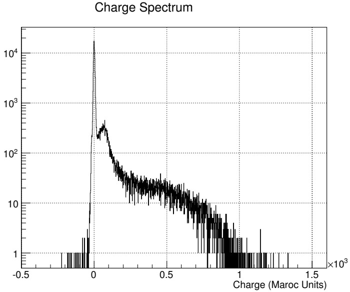


The H8500 single phe response function is too broad to perform a charge-based event-by-event reconstruction. Instead: perform a whole-spectrum analysis.

$$< N(Q_i) > = < E > \cdot LY \cdot G_i \cdot \varepsilon_i \cdot k_i$$

Normalize to the sum of the pixel averages:

$$\frac{< N(Q_i) >}{\sum_i < N(Q_i) >} = \frac{G_i \varepsilon_i k_i}{\sum_i G_i \varepsilon_i k_i} \Rightarrow \text{This can be compared with MC results for } k_i$$

# First measurements

The prototype response to a point-like $\alpha$ radioactive source ($^{241}Am$, $E = 5.49$ MeV) placed on the top face in different positions has been measured.

1. For each channel, the **charge** spectrum with and without the source has been measured
2. To obtain the "true" source spectrum: pedestal subtraction + background subtraction

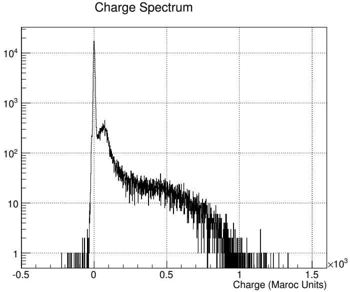


The H8500 single phe response function is too broad to perform a charge-based event-by-event reconstruction. Instead: perform a whole-spectrum analysis.

$$< N(Q_i) > = < E > \cdot LY \cdot G_i \cdot \varepsilon_i \cdot k_i$$

Normalize to the sum of the pixel averages:

$$\frac{< N(Q_i) >}{\sum_i < N(Q_i) >} = \frac{G_i \varepsilon_i k_i}{\sum_i G_i \varepsilon_i k_i}$$ ⇒ This can be compared with MC results for $k_i$

# Experimental results

$\alpha$ source at the center of the TOP face

Data Analytical model MonteCarlo

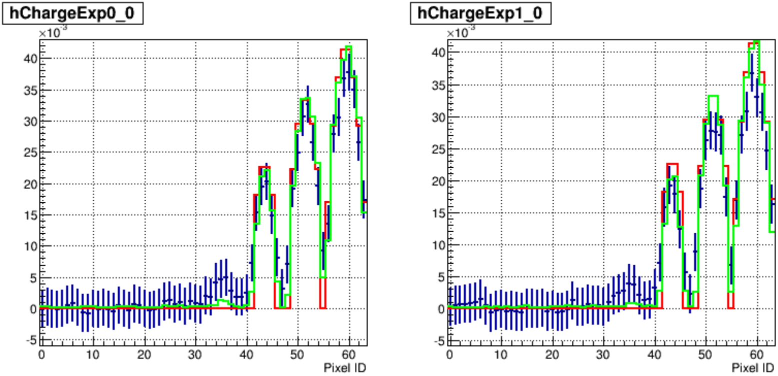

# Experimental results

$\alpha$ source in the opposite corner with respect to PMTs

Data Analytical model MonteCarlo

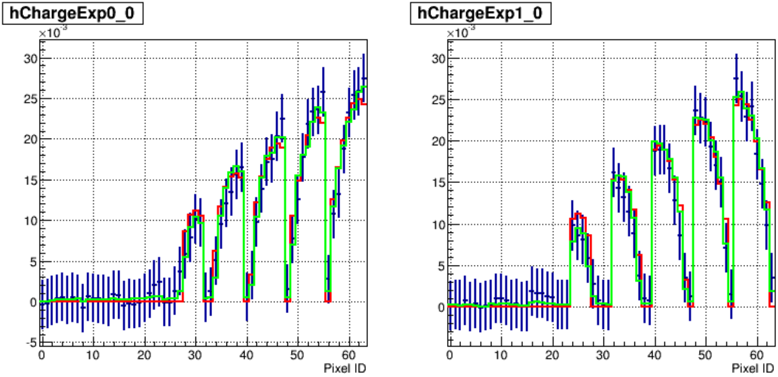

# Future activity

The obtained results will be used to design and construct a new prototype version, optimized for both photon count and hit-time measurements

- Photo-detector: MPPC array, S12642-008PB-50 or S13361-3050AE-08 (low-cross talk version)
- Readout: TOFPET[3]ASIC-based

The prototype response to radioactive sources, cosmic rays, and possibly $e^-$ beams (Frascati BTF) will be measured.

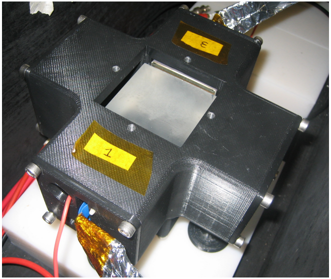

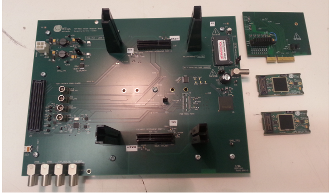

[3] JINST 8 C02050, 2013

Backup slides

# Project outline

Participants:

- A. Celentano (PI) - INFN Genova
- P. Boccacci - Unige DIBRIS
- D. Comoretto, M. Castellano - Unige DCCI

External collaboration:

- P. Musico, M. Turisini (FEE and DAQ)

Project details:

- INFN-Gruppo V project, call for young researchers
- Time frame: 2 years (Jan 2015 - Dec 2016)
- Budget: $\simeq$ 75+75 k€

# Reconstruction algorithms: alternative approach. Charge

## Point-like case

Isotropic emission of photons in the full solid angle (Poisson statistics) $\otimes$ Photons detection probability (Binomial statistics):

$$\log(\mathcal{L}_i) \propto N_i \log(\mu_i) - \mu_i$$

$$\mu_i = N_{tot} \cdot k_i(\vec{x}_P - \vec{x}_i) \cdot \varepsilon_i$$

- $k_i = \delta\Omega(\vec{x}_1 - \vec{x}_i)/4\pi$ : fraction of solid angle seen from the point $\vec{x}_1$ by the pixel at $\vec{x}_p$ [4]
- $\varepsilon_i$ : pixel quantum efficiency

## Trajectory case

Derived from the previous case, assuming uniform energy deposition along the trajectory:

$$\mu_i = \int_{\vec{x}_1}^{\vec{x}_2} d\vec{x}\, \mu_i(\vec{x}, N_{tot}/L)$$

Comparison between the analytic model and the MC prediction (point-like case):

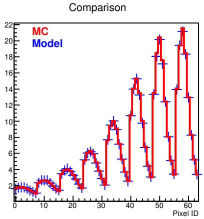


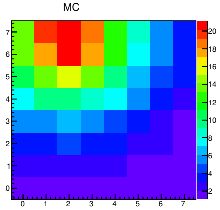


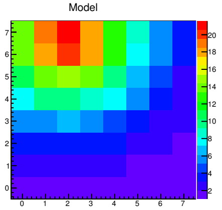


[4] I derived the formula for the general case of a rectangular surface arbitrary oriented.

# Reconstruction algorithms: alternative approach. Charge

## Point-like case

Isotropic emission of photons in the full solid angle (Poisson statistics) $\otimes$ Photons detection probability (Binomial statistics):

$$\log(\mathcal{L}_i) \propto N_i \log(\mu_i) - \mu_i$$

$$\mu_i = N_{tot} \cdot k_i(\vec{x}_P - \vec{x}_i) \cdot \varepsilon_i$$

- $k_i = \delta\Omega(\vec{x}_1 - \vec{x}_i)/4\pi$ : fraction of solid angle seen from the point $\vec{x}_1$ by the pixel at $\vec{x}_p$ [4]
- $\varepsilon_i$ : pixel quantum efficiency

## Trajectory case

Derived from the previous case, assuming uniform energy deposition along the trajectory:

$$\mu_i = \int_{\vec{x}_1}^{\vec{x}_2} d\vec{x}\, \mu_i(\vec{x}, N_{tot}/L)$$

Comparison between the analytic model and the MC prediction (trajectory case):

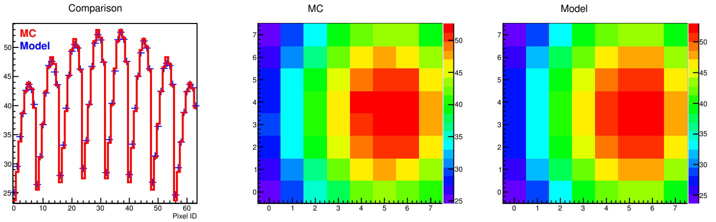


[4] I derived the formula for the general case of a rectangular surface arbitrary oriented.

## Reconstruction algorithms: alternative approach. Time

Involved functions:

- $p_s(t)$: Intrinsic scintillator photon-emission time PDF (exponential)
- $p_d(t)$: Detector intrinsic time-response function (gaussian)

**Point-like case:** spherical light source at $\vec{x}_0$

$$p_i(t) = p_s(t - t_0 - t_i) \otimes p_d(t - t_0 - t_i) \quad \Rightarrow \quad t_i = \frac{c}{n}|\vec{x}_i - \vec{x}_0|$$

**Trajectory case:** linear superposition of spherical light source between $\vec{x}_0$ and $\vec{x}_1$

$$p_i(t) \propto \int_{\vec{x}_1}^{\vec{x}_2} d\vec{x}\, n_i(t - t_0 - t^i_{\vec{x}})\, k_i(\vec{x}_p - \vec{x}_i) \quad \Rightarrow \quad t^i_{\vec{x}} = \frac{1}{\beta\, c}|\vec{x} - \vec{x_0}| + \frac{n}{c}|\vec{x_i} - \vec{x}|$$

**Geometrical interpretation:**

- "Top" detectors: first photon comes from $\vec{x}_1$
- "Bottom" detectors: first photon comes from $\vec{x}_2$
- "Middle" detectors: first photon comes from the $\check{C}$erenkov cone

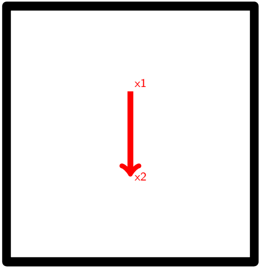

Involved functions:

- $p_s(t)$: Intrinsic scintillator photon-emission time PDF (exponential)
- $p_d(t)$: Detector intrinsic time-response function (gaussian)

**Point-like case:** spherical light source at $\vec{x}_0$

$$p_i(t) = p_s(t - t_0 - t_i) \otimes p_d(t - t_0 - t_i) \quad \Rightarrow \quad t_i = \frac{c}{n}|\vec{x}_i - \vec{x}_0|$$

**Trajectory case:** linear superposition of spherical light source between $\vec{x}_0$ and $\vec{x}_1$

$$p_i(t) \propto \int_{\vec{x}_1}^{\vec{x}_2} d\vec{x}\, n_i(t - t_0 - t^i_{\vec{x}})\, k_i(\vec{x}_p - \vec{x}_i) \quad \Rightarrow \quad t^i_{\vec{x}} = \frac{1}{\beta\, c}|\vec{x} - \vec{x_0}| + \frac{n}{c}|\vec{x_i} - \vec{x}|$$

**Geometrical interpretation:**

- "Top" detectors: first photon comes from $\vec{x}_1$
- "Bottom" detectors: first photon comes from $\vec{x}_2$
- "Middle" detectors: first photon comes from the $\breve{C}$erenkov cone

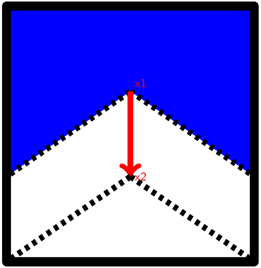

## Reconstruction algorithms: alternative approach. Time

Involved functions:

- $p_s(t)$: Intrinsic scintillator photon-emission time PDF (exponential)
- $p_d(t)$: Detector intrinsic time-response function (gaussian)

**Point-like case:** spherical light source at $\vec{x}_0$

$$p_i(t) = p_s(t - t_0 - t_i) \otimes p_d(t - t_0 - t_i) \quad \Rightarrow \quad t_i = \frac{c}{n}|\vec{x}_i - \vec{x}_0|$$

**Trajectory case:** linear superposition of spherical light source between $\vec{x}_0$ and $\vec{x}_1$

$$p_i(t) \propto \int_{\vec{x}_1}^{\vec{x}_2} d\vec{x}\, n_i(t - t_0 - t^i_{\vec{x}})\, k_i(\vec{x}_p - \vec{x}_i) \quad \Rightarrow \quad t^i_{\vec{x}} = \frac{1}{\beta\, c}|\vec{x} - \vec{x_0}| + \frac{n}{c}|\vec{x_i} - \vec{x}|$$

**Geometrical interpretation:**

- "Top" detectors: first photon comes from $\vec{x}_1$
- "Bottom" detectors: first photon comes from $\vec{x}_2$
- "Middle" detectors: first photon comes from the Čerenkov cone

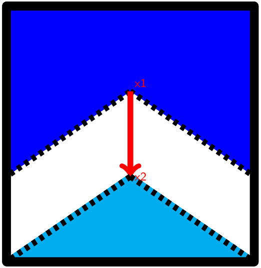

Involved functions:

- $p_s(t)$: Intrinsic scintillator photon-emission time PDF (exponential)
- $p_d(t)$: Detector intrinsic time-response function (gaussian)

**Point-like case:** spherical light source at $\vec{x}_0$

$$p_i(t) = p_s(t - t_0 - t_i) \otimes p_d(t - t_0 - t_i) \quad \Rightarrow \quad t_i = \frac{c}{n}|\vec{x}_i - \vec{x}_0|$$

**Trajectory case:** linear superposition of spherical light source between $\vec{x}_0$ and $\vec{x}_1$

$$p_i(t) \propto \int_{\vec{x}_1}^{\vec{x}_2} d\vec{x}\, n_i(t - t_0 - t^i_{\vec{x}})\, k_i(\vec{x}_p - \vec{x}_i) \quad \Rightarrow \quad t^i_{\vec{x}} = \frac{1}{\beta\, c}|\vec{x} - \vec{x_0}| + \frac{n}{c}|\vec{x_i} - \vec{x}|$$

**Geometrical interpretation:**

- "Top" detectors: first photon comes from $\vec{x}_1$
- "Bottom" detectors: first photon comes from $\vec{x}_2$
- "Middle" detectors: first photon comes from the $\breve{C}$erenkov cone

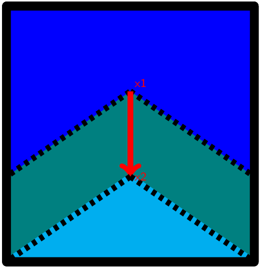

## MAROC3: 64-channel ASIC for MA-PMT readout

Features:

- Preamplifier, configurable (8 bit, $0 \ldots 4$)
- Fast line: 25 ns shaper + discriminator
- Slow line: 100 ns shaper + mem. cell
- Internal ADC (12 bit)

Outputs:

- 64x digital trigger signal
- Multiplexed analog charge
- Internal ADC digitized charge

Readout system:

- Original system developed for Medical Imaging with radionuclides
- 4096 channels, USB2.0 readout
- Internal trigger only (OR of all channels)
- No hit-time measurement

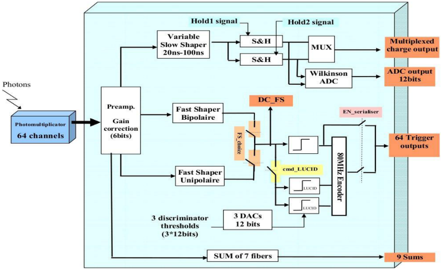


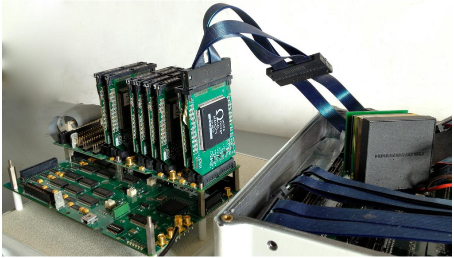

## Components R&D

The last part of the project ($\simeq$ last 6 months) will be devoted to a specific R&D program on the detector components.

**Develop a custom scintillator with optimized properties**

- Dope organic scintillators with a quencher, such as benzophenone ($Ph_2CO$), to lower the scintillation decay time[5].
- Develop wave-length shifting optical interfaces with organic molecules (for example, PVK).

**Use LA-PPD as photo-detectors**

State-of-the art photo-detectors, MCP-based, with micron-sized glass capillary arrays and ALD coating for functionalization. Performances:

- High gain: $G > 10^7$
- Extreme time resolution ($\sigma_t < 20$ ps single-phe)
- Very fine pixelization ($20\ \mu$m)

The project is currently in $R\&D$ phase: first samples (36 cm$^2$) available for tests in 2015.

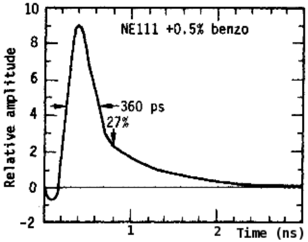


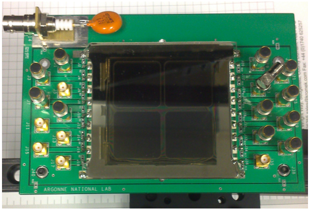


[5] IEEE Transactions on Nuclear Science 24.1 250-254 (1977)